Chapter 18
Comprehensive Design of Small Electric Vehicle for Powertrain Optimization for Optimum Range with Weight and Size Reduction

S. Vignesh, Yogesh Krishan Bhateshvar, Mohammad Rafiq B. Agrewale, and K. C. Vora

Abstract Installing Small Electric Vehicle (SEV) in India can potentially act as substitute for taxi/cabs in urban areas where new vehicles can't be deployed considering traffic and stringent emission norms proposed by the government. To expedite this, a quadricycle is benchmarked for retro-fitment and new design is proposed for purpose-built SEV including floor mounted battery pack. Modular electric platform is also investigated with various iterations in powertrain including the front and rear mounting possibilities of motor and battery pack, respectively, for retro-fitted one. Structural stress analysis is performed to find out the maximum possible weight of the battery pack to fit on the floor for purpose-built one. The concept design has a tubular structure for chassis and materials for the chassis are varied to mount the battery pack of weight 200 kg on the floor of SEV. The design of experiments is done on chassis materials for estimating the lowest possible curb weight of SEV. Based on modular battery pack design, a maximum of 23% weight reduction is possible following the curb weight of the Internal Combustion (IC) engine variant of the benchmarked small passenger car. In electric motor, the parameters of interest are motor speed, motor torque and motor efficiency where altering the number of poles leads to maximization in SEV performance. Vehicle parameters such as maximum speed, vehicle acceleration, final drive gear reduction ratio, and battery pack current are compared with the energy economy of the small electric vehicle. The battery pack is designed to fit under the front hood of the vehicle, whereas the motor is fitted at

S. Vignesh (✉) · M. R. B. Agrewale · K. C. Vora
Automotive Engineering, ARAI Academy, Pune, India
e-mail: vickykpm09@gmail.com

M. R. B. Agrewale
e-mail: rafiq.pga@araiindia.com

K. C. Vora
e-mail: vora.pga@araiindia.com

Y. K. Bhateshvar
ARAI Academy, Pune, India
e-mail: bhateshvar.pga@araiindia.com

A. K. Bohre et al. (eds.), *Planning of Hybrid Renewable Energy Systems, Electric Vehicles and Microgrid*, Energy Systems in Electrical Engineering,
https://doi.org/10.1007/978-981-19-0979-5_18

the rear. The driving range is estimated using Simulink and it is validated with mathematical calculation using Peukert method performed in MATLAB. It is concluded that the designed vehicle with Switched Reluctance Motor (SRM) 6/4 configuration of 15 kW, 110 Nm is showing enough capability on the replication of urban car in 2020 targets. For the betterment of range, NCA chemistry is preferred over other lithium-ion chemistries. This chapter provides a complete look of electric powertrain for SEV and its design characteristics through retro-fitted and purpose-built one and its application where electric mobility can be installed seamlessly.

Keywords Small electric vehicle · Retro-fitment · Purpose-built · Concept chassis · Switched reluctance motor · Battery swapping · Driving cycle · Range

Nomenclature

SEV	Small Electric Vehicle
SRM	Switched Reluctance Motor
kg	Kilo gram
LFP	Lithium Ferrous Phosphate
CFRP	Carbon Fiber-Reinforced Plastic
C_D	Drag coefficient
CO_2	Carbon dioxide
HWFET	High Way Fuel Economy Test
SOH	State of Health
NASA	National Aeronautics and Space Administration
LMO	Lithium Manganese Oxide
LCO	Lithium Cobalt Oxide
NEDC	New European Driving Cycle
NYCC	New York City Cycle
WLTP	Worldwide Harmonized Light vehicle Test Procedure
PMSM	Permanent Magnet Synchronous Motor
DC	Direct Current
CVT	Continuous Variable Transmission
GA	Genetic Algorithm
Ah	Ampere hour
MEET	Mahle Efficient Electric Transport
PHEV	Plugin Hybrid Electric Vehicle
ANSA	Automatic Net generation for Structural Analysis
IC	Internal Combustion
NCA	Nickel Cobalt Aluminum
BIW	Body in White
EV	Electric Vehicle
EPA	Environmental Protection Agency
SAE	Society of Automotive Engineers

UDDS	Urban Dynamometer Driving Schedule
SOC	State of Charge
BMS	Battery Management Systems
NMC	Nickel Manganese Cobalt
LTO	Lithium Titanate Oxide
TCO	Total Cost of Ownership
ISO	International Standards Organization
LA	Los Angeles
BLDC	Brush Less Direct Current
ECE	Economic Commission for Europe
AMT	Automated Manual Transmission
DCT	Dual Clutch Transmission
CNG	Compressed Natural Gas
SUV	Sports Utility Vehicle
EU	European Union
UNECE	United Nation Economic Commission for Europe
AISI	American Iron and Steel Institute

18.1 Introduction

Floor battery packs are quite common in electric vehicles. The battery pack is usually mounted in between front and rear axle for making provisions of skate board-type electric vehicle chassis architecture. There is enough ground clearance given in mounting the battery pack on the floor. Due to this, the wheelbase tends to be longer and hence the cars have lower ground clearance (Luccarelli et al. 2014). In general, the weight of the Body in White (BIW) is in the ratio of 1:4 times the curb weight of the vehicle. For example, the Renault concept has a curb weight of 800 kg and its BIW weighs 200 kg (Lesemann et al. 2013). Tesla introduced the skateboard type of arrangement where the motor is mounted on either the front or rear axle depending on the drive train configuration. The battery pack is mounted in between the front and rear axles. SEVs have a smaller wheelbase than full-size sedans. But due to lack of literatures on scalable battery pack the research is very few. Hence, this chapter brings out the need of scalable battery pack in SEV.

The chapter is organized in the following sequence as given in Fig. 18.1. SEV preparation from the scratch requires the material selection for the chassis needs to be done followed by the projected weight of the chassis and its stress analysis and corresponding mathematical validations. Road load coefficients and its significance on distance traveled by the SEV is studied. In SEV, installing a battery pack which caters a minimum of 200 km range is tedious task considering the volume availability. Hence, this chapter also deals with the proposal of modular design of battery packs which can be scaled according to powertrain requirements. In addition to this, battery chemistry for lithium ion (Lithium Ferrous Phosphate (LFP),

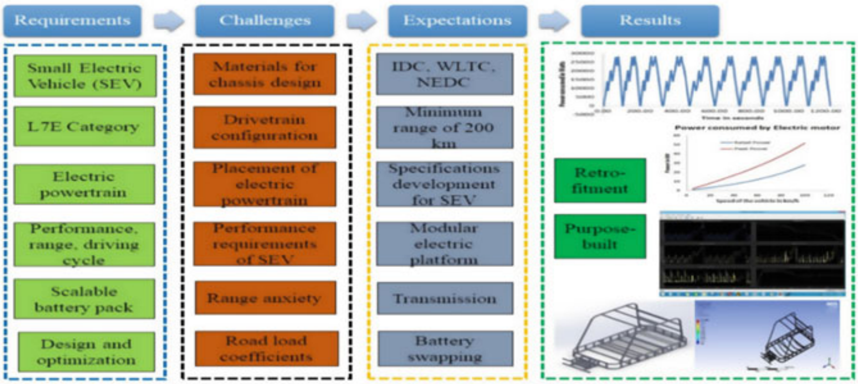

Fig. 18.1 Graphical abstract

Nickel Cobalt Aluminum (NCA)), metal air, lithium polymer, lead acid, and nickel metal hydride were considered for range estimation of the proposed SEV. This is followed by the implementation of reduction ratio to the drive axle by including the power transmission concepts applicable to electric vehicle. Motor operating voltage will have significant contribution in altering the performance of an electric vehicle. Hence, the reduction ratio applicable for various operating voltages is studied for the proposed SEV. Battery pack optimization is carried out based on the volume availability, specific energy catered by the battery pack, and expected range to be delivered by the vehicle. Once the powertrain specification is finalised for the proposed SEV, vehicle level simulation is carried out in EV reference application from MATLAB/Simulink for range estimation and performance monitoring at different driving cycles. The whole outcome of this chapter is to study the significance of modular electric powertrain design possibilities for the SEV under various iterations proposed on the battery pack. Based on this analysis, it is observed that a quadricycle can fulfil the urban mobility requirements when considered for electrification and offers a minimum range of 200 km when SRM 6/4 configuration is preferred with lithium-ion battery pack with NCA composition. The contribution and novelty of the proposed work are as follows:

- Mathematical model for the benchmarked vehicle for retro-fitment and purpose-built one.
- Concept design for purpose-built SEV chassis and its structural stress analysis.
- Empirical analysis of road load coefficients corresponding to small electric vehicle.
- Modular electric platform proposal with 48, 72, and 192 V system voltage and its corresponding gear ratio requirements.
- Scalable battery pack configuration in purpose-built SEV.

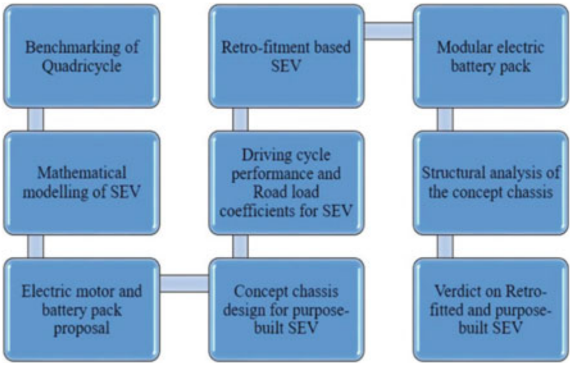

Fig. 18.2 Flow of work in this chapter

- Powertrain behavior of the proposed SEV through driving cycle Indian Driving Cycle (IDC), NEDC (New European Driving Cycle), Worldwide Harmonized Light vehicle Test Procedure (WLTP).

The flow of the proposed work is given in Fig. 18.2.

18.2 Materials for SEV Chassis

Mass of the chassis is an integral part of the curb weight of electric vehicles. In the past, chassis members are flexible. Now there is an increase in structural rigidity that demands good structural stiffness and excellent material properties. Lowering the weight of the chassis reduces inertia and simultaneously the performance of the vehicle can be improved. Ladder chassis is used in heavy vehicles and space frame (the tubular structure is preferred) is used in recent days. Chassis generally designed to keep a 200 kg battery pack on the floor. The wheelbase of 1800 mm is pre-determined to fix the length of the vehicle as 2700 mm for quadricycle having two seats. The width of the chassis is 1515 mm. It is made up of American Iron and Steel Institute (AISI) 1020 and the weight of the chassis is 84 kg (CarlosGertz et al. 2014). Stress analysis of the ladder frame is carried out using the finite element method. Alloy steel is preferred again which has a yield strength of 620 Mpa. This chassis is designed to carry 860 kg of load including motor, battery, passengers (Kristyadi et al. 2017). AISI 1018 is preferred for electric car chassis which has an ultimate strength of 634 Mpa. Chassis is analyzed for the payload of 1.5 kN. Moreover, it withstands 70 kg of the load before the actual deformation occurs (Taufik et al. 2014). The structural modifications in the chassis can be carried out by modifying the double ladder in to single ladder. But it requires the suspension should be connected strongly to the chassis made up of mild steel. One tonne of weight load applied on the carrier of the electric vehicle which is intended to carry goods, 1200 N is applied to the driver's cabin, and 300 N is applied to the battery pack region (Arun et al. 2019). Materials allocated for electric vehicle chassis can be steel, alloy steel, aluminum.

Lightweight chassis requires the material should have high yield strength at the same time low density. Aluminum is a recent entrant in the automobile industry where it is used to make body panels, bumpers. Al 6061 T4, Al 6063 T4 can be used to design the chassis for the electric vehicle. The factor of safety is pivotal in the sense of an increase in the factor of safety increases the cost of productivity. Hence, generally the factor of safety is kept between 1 and 2. If the factor of safety is low then deformation of the chassis is likely to be high (Koumartzakis et al. 2017).

Quadricycles belong to L7E offers a minimum of 150 km range with 16 kWh. When it comes to drivetrain, the requirements are as follows:

- Vehicle weight of less than 600 kg.
- Vehicle acceleration of 0–100 km/h in 10 s.
- Electric range more than 150 km.
- The energy efficiency of less than 80 Wh/km.

Based on this target, vehicle weight holds the key factor if there is a compromise between performance and range. Carbon Fibre-Reinforced Plastic (CFRP) Al space frame structure is used in the Epsilon quadricycle concept (Stein et al. 2016). While selecting the alloy steels, the ultimate strength should be given more importance. A vehicle that weighs 420 kg is designed in CATIA V5 R 18 and stress analysis is carried out using structural alloy, magnesium alloy, and aluminum alloy. Out of these three, magnesium weighs the lowest courtesy low density. It is observed that the weight of the chassis downs by a factor of 4 when it is made of magnesium alloy than steel. One hundred and seventy-five kilograms are allocated for the battery pack. The factor of safety considered is 1.25 stress values are lesser in magnesium alloy (Singh and Chauhan 2017).

Battery pack voltage is a major contributor in deciding the width of the battery pack. Packaging issues are severe when the battery pack voltage is higher. Subsequently in SEV, the floor battery pack is tedious when the chassis structure is monocoque. This is one of the major obstacles for retro-fitment of an electric vehicle with a floor battery pack. The modular design of the battery pack allows the battery pack voltage can be scalable according to the vehicle requirements. The space frame structure is more flexible than monocoque hence it is always preferred for scalable battery packs (Patel and Kumar 2017). Crashworthiness demands more strength from electric vehicle chassis in the event of a crash. High-performance composite materials can be used as chassis materials (Wismans et al. 2011).

Some of the electric vehicles are dedicatedly designed for racing applications. Shell Eco-Marathon is one such race where the electric vehicle is designed according to the guidelines given in the Shell Eco-Marathon competition. At the rear end AISI 9000 steel is used and Aluminum 6082-T6 series is preferred. Automatic Net generation and Structural Analysis (ANSA) pre-processor is used in solving the finite element model (Tsirogiannis et al. 2019).

Due to the increase of traffic in cities, shared mobility is touted as the successor among personal vehicle usage. Recent advancements in shared mobility concepts merged OLA with Mahindra for producing electric vehicles that can be used for urban mobility. The modular vehicle weighs 500 kg. A 30 kW electric motor is used which has a peak power of 90 kW. Battery capacity is 4.62 kWh and has a voltage of 77 V (Maryniuk 2017). This chassis is benchmarked for the concept design in this paper.

Hu-Go is a quadricycle which weighs 257 kg including batteries. Its energy consumption is 51 Wh/km whereas Renault Twizy consumes 70 Wh/km though placed in the same L7E category. With reduced weight, the battery capacity required is just 5.1 kWh for a 100 km range. Space constraints can be addressed by mounting the batteries on the floor (Tanik and Parlaktaş 2015).

18.3 Road Load Coefficients

Chassis dynamometer is an equipment used to measure the road load forces associated with the vehicle prone to testing where simulation of actual road profile is also possible. The results of this test give three coefficients say A, B, and C or in some works of literature it is mentioned as F0, F1, and F2. Also, there will be deviations in the vehicle specifications when the tests are carried out for getting type approval and the tests carried out in an actual vehicle. Coast-down tests are performed in order to measure car's total load. The outcomes of the coast-down test is used to predict the car's fuel economy and later it can also be used for certification purposes. The term road load can be termed as the force needed to propel at constant speeds from neutral gear on a given flat road.

Driving cycles are used to quantify the car's emission level and fuel consumption on a roller test bench. This bench consists of a dynamometer that caters driving experience applicable on a real road. The key aspect on roller test bench is that force acting on the dyno (F_{dyno}) is not equal to the force acting on the vehicle ($F_{vehicle}$). The real-time loads acting on the vehicle can be simulated by the rollers in a test bench. Usually, the resistance of the car is taken as twice in order to include vehicle losses (Norrby 2012).

18.3.1 Significance of Road Load Coefficients

The driving range of electric vehicles varies according to traffic conditions, driving cycle, rolling resistance, aerodynamic resistance, slope angle, and wind speed. If the car satisfies United Nations Economic Commission of Europe (UN ECE) 101 standards, then the vehicle is termed as a pure electric vehicle. Courant is the passenger vehicle, based on the standard version of the engine ignition. Battery charging time is 12–14 h. The economical speed to get 150 km range is 40 km/h, whereas the maximum speed is 85 km/h (Gis et al. 2012). When the vehicle is tested for fuel economy it is recommended to estimate the aerodynamic, gradient, rolling loads associated with the vehicle. Failing to do so leads to a violation of the Environmental Protection Agency (EPA) norms. Dynamometer settings are of two types. The first one deals with the estimation of road load forces under controlled test conditions. The second one involves the determination of deviations between on-road tests and chassis dynamometer tests. In other words, the second one encompasses the correction factor to compensate for the deviations between actual and simulated ones (Determination and Use of Road Load Force and Dynamometer Settings 2015). The fuel economy of an electric vehicle can be enhanced by decreasing the weight of the vehicle. Rolling resistance can be reduced by installing tires with lower rolling resistance coefficient. The value 0.009 seems to be ideal but in practical 0.011–0.015. Aerodynamic resistance can be reduced by reducing the coefficient of drag (C_D). C_D value of 0.25–0.3 seems to be perfectly aerodynamic one even though the cars whose C_D is less than 0.25 is also available in the market (Kühlwein 2016).

Coasting the vehicle is possible using the vehicle's kinetic energy. The equation of motion for deceleration is given by

$$m \cdot b \cdot \delta = -F_b \tag{18.1}$$

where m is the mass of the vehicle (kg).

b is the deceleration (m/s^2).

δ is the rotational inertia (1.03–1.04 times the mass of the vehicle).

F_b is the braking force (N).

The braking force is given by

$$F_b = G_v \cdot f \cdot \cos\alpha \pm G_v \cdot \sin\alpha + \frac{1}{2}\rho C_D A \cdot v^2 \tag{18.2}$$

where G_v is the vehicle gravitational force.

f is the rolling resistance coefficient.

α is the slope angle.

ρ is air density (kg/m^3).

C_D is the aerodynamic drag coefficient.

A is the vehicle frontal area or projected area (m^2).

v is the velocity of the vehicle (m/s).

When the vehicle is moving up the gradient, the gradient resistance is positive and vice versa for moving down the gradient (Barta et al. 2018).

While predicting the range of electric vehicles, the accuracy is of prime importance. Simulation software is employed to estimate the vehicle performance, fuel economy, and emissions tests. Such software is often used to reduce the cost instead of building prototypes to carry out the tests. Those tests were performed on Mitsubishi i-MEV, BMW i3, Nissan leaf EV, and Ford Focus EV. The road load coefficients of the same are estimated through chassis dynamometer tests and the results were compared with the simulation of such tests performed in ADVISOR (Humphries and Morozov 2016). Theoretical estimation of the coast down coefficients are also possible with certain vehicle dynamics equations. Data acquisition systems are used in coast-down tests. Acquisition errors along with errors in wind speed, road slope are the reasons for poor accuracy in coast-down results (Preda et al. 2010). Fuel consumption is usually notified in terms of litres per 100 km and CO_2 emissions are given in grams per litre. While simulating the vehicle on a roller test bench, vehicle speed is the key factor. This is performed based The road load curve gives the measure of vehicle performance. Hence, the estimation of road load curve is crucial in compliance with legislative norms (Kadijk 2012). Hence, there exists type approval and realistic specifications of the test vehicle.

18.4 Modular Battery Pack Design

Battery capacity is not the only factor that influences the range of the electric vehicle. In addition to that vehicle weight, the size of the electric motor also plays an instrumental role in determining the range of electric vehicles (Mruzek et al. 2016). Society of Automotive Engineers (SAE) J1263 norms were followed while conducting road load estimation tests. The atmospheric temperature should fall in the range of 5°–38° C. Minimum five runs should be conducted and the weighted average is taken for road load coefficients (Wishart and Diez 2015). The default driving cycle will be Urban Dynamometer Driving Schedule (UDDS) and High Way Fuel Economy Test (HWFET) according to SAE J1634. Dynamometer tests are conducted according to SAE J1263 (Implementation of SAE J1634 1997). In this paper while estimating the braking distances, thinking distance, and stopping distance is calculated at speeds in 10 km/h increments (https://www.highwaycodeuk.co.uk/answers/what-is-the-stopping-and-braking-distance-of-a-car).

Most of the vehicles built today are of monocoque chassis structure, where the body and chassis are unitized together. When mounting batteries on the floor, this type of chassis is not recommended for SEV. Therefore, there is a need to propose the front and rear mountable battery pack for SEV's.

The modularization of battery packs is the need of the hour in the electric vehicle segment. The motors selected for an electric vehicle has unique voltage requirements. Hence, to satisfy motor voltage, the battery pack should be scalable enough. Apart from basic design requirements, the cost and the life of the battery pack are the other parameters that decide the suitable battery pack. The battery pack should possess better heat transfer characteristics. The influential parameters apart from heat transfer are the design of the battery thermal management system and packaging architecture (Arora et al. 2018). Hence, there is a need for suitable battery architecture which supports the space available in SEV.

Lead–acid batteries are cheap and mature technology. Lithium-ion has several advantages than lead–acid in terms of specific energy and energy density (May et al. 2018). Lithium-ion drives the battery market today extensively for electric vehicles other than batteries for laptops, mobile phones. When it comes to the electric vehicle, the range is the primary factor. Low cost and long life are the secondary factors that drive in synchronous with electric vehicle promotion in urban mobility. The willingness to pay ratio for the additional range is very low in India compared with emerging countries. Because of space constraint and lower specific energy of lead–acid and nickel metal hydride, they are not preferred in SEV's. Hence, the potential customers to support range, low cost, and higher specific energy are lithium–sulfur, zinc-air. Cost-wise lithium–sulfur is cheaper than zinc-air. Metal-air batteries possess the capability of catering higher range than current lithium-ion battery technology. It is projected that lithium–sulfur seems to be an ideal replacement for lithium-ion, whereas metal-air batteries are still in the developing stage (Cano et al. 2018). When the electric vehicle is in use, the battery pack life deteriorates over a period. There the discussion about the second use of batteries is valid. However, due to the lack of literature about used batteries and its applications such as grid connectivity, stand-alone houses the life cycle analysis is not enough to predict the best battery pack (Bobbaa et al. 2018).

Battery performance is measured by the State of Charge (SOC), State of Health (SOH), and the number of life cycles possible in the battery before it starts to degrade. Cell-to-cell variations has to be analyzed since small changes exist in the cell that can be identified easily by the Battery Management System (BMS) (Dubarry et al. 2018). Gaussian model is available to predict the battery SOC, SOH with a root mean square value of 4.3%. National Aeronautics and Space Administration (NASA) Randomized battery sheet is used for primary data about the battery datasets (Richardson et al. 2018). Zinc-air battery can be used as a secondary power source for lithium ion. It has a longer life span than lithium ion (Sherman et al. 2018). Increasing the battery capacity of a battery pack certainly reflects an increased weight of the electric vehicle. The energy economy can be expressed by the number of Watt-hours required to travel unit km. The economic vehicles were Renault Twizzy (67.8 Wh/km), Tazzari Zero (87.9 Wh/km), and Renault Zoe ZE22 (93.6 Wh/km). Currently, Tesla Model S has a longer range courtesy to 100 kWh battery pack which weighs 600 kg. The battery pack weight is almost equal to the curb weight of SEV. However, the energy consumption of the Tesla Model S is 199.5 Wh/km. Hence, the battery pack weight influences the range of electric vehicles (Berjoza and Jurgena 2017). The battery chemistries of lithium ion involved in automotive applications are Lithium Ferrous Phosphate (LFP), Lithium Nickel Cobalt Aluminum (NCA), Lithium Nickel Manganese Cobalt (NMC), Lithium Manganese Spinel (LMO), and Lithium Titanite (LTO). The prominent chemistry in consumer applications is Lithium Cobalt Oxide (LCO). Out of the various lithium chemistries, LFP and NMC have a good balance in terms of cost, safety, specific power, specific energy, life, and performance. A 15 kWh battery pack is common in India. The cost of a 15-kWh battery pack in 2018 is reduced by 65% when compared with the cost in 2009. Further, the infrastructure required for charging the electric vehicle is in the development stage and hence while charging the electric vehicle, a part of infrastructure costs are also added to the customer. Research is still in progress, on reducing the Total Cost of Ownership (TCO) of electric vehicles (Dinger et al. 2010). Even though lithium-air has a higher theoretical specific energy of 3458 Wh/kg, achieving this in practice is difficult. It is projected that urban cars in 2020 will be having 675 kg curb weight, having a battery weight of 175 kg which fuels up to 225 km. This equates to 500 kg weight is distributed between BIW, Motor, Transmission system, and miscellaneous components in the electric vehicle. In developing countries, SEV's play a pivotal role in shifting to electric mobility. Currently, lithium-air batteries have a lower depth of discharge of 1000 mAh/g and lithium–sulfur is closer to industrialization since the C-Rate matches with lithium-ion (Lampic et al. 2016). The driving pattern of electric vehicles can impact the range as visualized by a 30% decrement in energy consumption for the NEDC driving cycle when the operating point is tilted towards the economy. Soon lithium–sulfur is one of the battery packs which propel electric vehicles (Othaganont et al. 2016).

To improve the range, battery pack design is the main factor. Employing a 24-kWh battery pack in the electric vehicle for a 50 km daily commute is like investing the surplus amount of energy into it. Hence, the appropriate size of the battery pack proposed for the right purpose makes electric vehicles successful. In modularization, the customer decides the capacity of the battery pack according to their commute (Mruzek et al. 2014). In India, a study was conducted on electric vehicle road maps and scenarios. The key findings include:

- Battery technology is gearing up for drastic improvement which involves cost reduction and improved specific energy.
- Electric 2 wheelers and cars are comparable to conventional vehicles, but lack of charging infrastructure is still a concern.
- Transport demand is expected to improve soon.
- Higher penetration of electric vehicles increases electricity demand (Shukla et al. 2014).

18.5 Energy Economy in Electric Vehicles

Electric vehicle range can also be referred as energy economy of the vehicle. When the vehicle is being tested, the parameters such as pressure, temperature, and velocity are influential in determining the fuel economy of the vehicle according to the standards published by SAE, ISO. The real-time ambience is completely different when compared to the testing standards and testing conditions. In such cases, there is a variation in the driving range is observed between the real-time conditions with respect to the tested ones under controlled conditions. In order to predict the fuel economy of the vehicle under such conditions requires an engineering model to be proposed, especially for the controlled testing conditions. O. Karabasagolu et al. used UDDS, US-06, HWFET, NYCC, and LA-92 driving cycles in order to predict the fuel economy. (Karabasoglu and Michalek 2013). Specific energy consumption of a four-seated passenger car lies around 84 Wh/km. Though the driving cycle is varying with respected to the testing conditions, it will vary the energy consumption of the vehicle. For a low-powered passenger car (power <10 kW), the range of 70–95 km is obtained at various driving cycles with the maximum speed being 117 km/h and usable battery pack capacity of 6.54 kWh (Saxena et al. 2020). In the case of urban mobility, the range of 100 km is still hovering due to electrical accessories usage consumption. Design criteria do matter a lot when it comes to low-speed or high-speed vehicle applications. Thus, the performance parameters such as maximum speed, torque, gradient, and vehicle acceleration varies according to the driving cycles (Barlow et al. 2009). Chassis dynamometer offers testing at vehicle level and also it caters a good validation by simulating the on-road conditions. Testing agencies do follow different protocols for vehicle testing along with its validation (Type I test On S.I. engines, CNG, LPG and diesel engine vehicles (Verifying the average tailpipe emission) of gaseous and particulate pollutants 2018). Increment in battery capacity will lead to increment in battery pack weight. The specific weight coefficient of the battery pack is given by

$$K = \frac{m_{\text{batt}}}{m_{EV}} \tag{18.3}$$

where, K is the specific weight coefficient,

m_{batt} is the mass of the battery pack (kg),

m_{EV} is the mass of the electric vehicle (kg).

Renault Twizzy has specific weight coefficient of 67 Wh/km, whereas Tesla Model S has specific weight coefficient of 199 Wh/km (Berjoza and Jurgena 2017). Driving cycle testing time and distance will have a significant call over CO_2 emissions (Ciuffo et al. 2017). World Harmonized Driving Cycle can be supported in having a common driving cycle which shall be considered in all terrain and driving conditions (Tutuianu et al. 2014).

A small electric vehicle having a weight of 800–900 kg is supported by a 30 kW SRM having a peak torque of 110 Nm was explored by S. Kachapornkul et al. (Kachapornkul et al. 2007). This paper closely follows the powertrain requirements fixed by S. Kachapornkul et al. Since the speed requirement is different for various driving cycles, SRM only fulfills the maximum speed criteria among BLDC, PMSM. This led to the finalization of electric model having SRM with 15 kW nominal and 30 kW peak power requirements. Battery placement is often being front hood or rear hood in SEV. Since the motor is mounted on the rear axle, the rear wheel drive configuration is preferred in mass production. LFP cells of three layers (18,650) shown in Figs. 18.1 and 18.2; 86.4 Ah, is placed in three layers under the front hood. Considering an SEV, the maximum car width is having around 1.5 m of width for battery pack placement. Driving cycles are altered using simulink platform where the battery capacity of 13.264 kWh is usable from a pack capacity of 16.58 kWh.

18.6 Electric Vehicle Transmission

Electric vehicle is gaining much attention in the automotive industry. Majority of the vehicles have single stage reduction ratio. The motors used in the vehicle have the sufficient thrust to propel basic needs of an automobile. It is the transmission system which makes the motor to operate in optimum speed and the vehicle speed can be matched to meet the driving requirements (Hofman et al. 2016). Multi-stage transmission will improve the energy economy but the vehicle purpose has to be clearly defined. It widens the range of electric vehicle operating zone. Transmission system acts as torque amplifier for electric vehicles. Motor controller is of prime importance in such a way that drivability can be improved (Zhou et al. 2012). IC engines requires gear box to amplify the torque requirements since the torque is comparatively low when compared with electric motors. Reduction ratio depends on the vehicle application and road profiles. By 2030, it is forecasted as 41% of battery electric vehicles will be on the road across the globe (https://www.ngevehicles.com/ev-technical/driving-into-2025-the-future-of-electric-vehicles.html).

18.6.1 Background in Transmission System

Two-speed transmission systems are becoming popular recent days due to their improved energy economy over single-speed one. Vehicle parameters such as mass, drag coefficient, gradient, and frontal area are instrumental in determining the power required by the motor. Battery pack defines the finite distance traveled by the vehicle in between two successive charging. Two-speed transmissions have better energy economy than single stage one. For small electric vehicles, single-speed transmission is enough to meet the driving requirements (Lu et al. 2017). Driving cycle contributes a significant part to the vehicles energy economy. Economic Commission of Europe (ECE) R 15 is such a cycle defined for urban mobility has a maximum speed of 50 km/h. Vehicle parameters can be fixed through driving cycle. The power consumed by the motor for propelling the vehicle on a gradient requires the power to be catered over a period of time. Hence, the motor should be capable of providing the required thrust for a period of time. For small electric vehicles, it is better to choose the motor with lower nominal torque and short time overloading (Prochazka et al. 2015). Downsizing of the motor and battery pack can be possible only if the vehicle have good transmission system. It indirectly correlates to the need of multiple speed transmission system. Vehicle kerb weight is also one of the deciding factors that assume the need of multiple speeds (Chander et al. 2018). Motors can generate maximum torque at low speeds and it can propel the vehicle at rest with ease than IC engine. Most of the small electric vehicles are coupled with single-speed transmission. Two-speed transmission systems can improve the functionality of DC motor-based traction system. Thus, the motor selection for small electric vehicle is critical here (Mahala and Deb 2011). Small electric vehicles sales are quite high in foreign countries like Japan, South Korea, etc. In small passenger cars segment, Nissan leaf and Renault ZOE are popular. BMW is selling smaller electric vehicles first before stepping in to SUV's and sedans but Audi and Mercedes have their own platform (https://www.ngevehicles.com/ev-technical/driving-into-2025-the-future-of-electric-vehicles.html). The automatic transmissions currently used in electric vehicles include Automated Manual Transmission (AMT), Dual Clutch Transmission (DCT), and Continuously Variable Transmission (CVT). Optimization of gear ratios can be done through Genetic Algorithm (GA) approach (Yin et al. 2017). For small electric vehicles, single-speed transmission is typical assumption. Multi-speed transmission is not recommended due to increased weight and cost (Faid 2015). Small electric vehicles have lower reduction ratio and torque from the motor is maximum. This increases the size of the motor to a certain extent. In the same page, increasing the reduction ratio to a larger value increases motor speed and power loss also increases by a margin (Isobe et al. 2011). Mileage of electric vehicles ranges from 110 to 480 km based on the battery capacity installed. In small electric vehicles the space availability of keeping the batteries is low. Motor characteristics are important in defining the reduction ratio of small electric vehicle. To ensure top speed the reduction ratio of the vehicle is kept small and making the motor to run at its maximum efficiency. The final drive ratio will be in the range of 1–4 for such small reduction ratios (Xin and Chengning 2017). Higher the speed of the vehicle, it is recommended to keep multiple gear ratios for the IC engine powered and electric vehicles. If the purpose of vehicle is meant for urban mobility, then higher speeds are not recommended. Hence, single-speed transmission is justifiable at this moment (Parkinson 2016).

18.7 Motor Voltage and Transmission-Related Optimization for SEV

In this paper, benchmarking is carried out on small passenger car. It is converted to motor powered vehicle by defining the power required by the motor. Battery calculations are performed by keeping the constraints of battery weight less than 150 kg and space availability in the front and rear boot. Retro-fitment is given higher importance hence the battery pack has to be placed either at the front or at the back. The motor voltage is varied for 48, 72, and 192 V operating system. Gear ratio is changed accordingly by keeping the maximum torque of the motor to match with Indian Driving Cycle requirements. Analysis is carried out for the small electric vehicle moving on flat road as well as at a constant gradient of 5°. This value is much higher than what is declared in the driving cycle. Even in driving cycles also the maximum gradient is applicable for finite amount of time.

Motor selection is based on rated power and peak power required by the small electric vehicle. Voltage is adjusted by matching the gear ratio with the driving cycle requirements. It is followed by the analysis of instantaneous motor voltage, torque, speed, and current for the driving cycle imposed. Battery pack is proposed for lithium ion cylindrical cell having LFP chemistry. Weight of the battery pack is compared for the motor voltages defined in this paper. Weight distribution is given higher importance since retro-fitment is proposed.

The specifications of small gasoline passenger car are given below:

- Power = 9 kW
- Engine = 220 c.c. single cylinder

- Fuel economy = 35 km/l for petrol and 43 km/kg for Compressed Natural Gas (CNG)
- Kerb weight = 450 kg
- Max speed = 70 km/h
- Dimensions = 2752 × 1312 × 1652 mm
- Projected area = 2.16 m^2
- Wheel base = 1925 mm
- Wheel track = 1143 mm
- Turning circle Radius = 3.5 m
- Front storage capacity = 60 L
- Center storage capacity = 95 L
- Rear storage capacity = 44 L
- CO_2 emitted = 66 g/Km
- Tyre size = 135/70 R12 Tubeless.

For converting this benchmarked vehicle to electric one, tractive effort calculations are carried out.

18.7.1 Rolling Resistance

$$F_r = f_r mg \cos\alpha \tag{18.4}$$

f_r is rolling resistance coefficient of tyre;
g is acceleration due to gravity (m/s^2);
α is road slope (rad);
Rolling resistance coefficient = 0.0136 × (0.40 × V^2 × 10^{-7});
Coefficient of friction = 0.4 and 0.7 for wet and dry roads;
f_r = 0.0137 for wet roads and 0.0139 for dry roads;
m = 719 kg;
g = acceleration due to gravity = 9.81 m/s^2;
Rolling resistance = 0.0139 × 719 × 9.81 = 96.631 N.

18.7.2 Aerodynamic Resistance

$$F_{\mathrm{air}} = \frac{1}{2}\rho C_d A_f (v)^2 \tag{18.5}$$

ρ is the air density (Kg/m^3);
C_d is the aerodynamic drag coefficient;
A_f is the frontal area;
v is the vehicle speed (m/s);
C_d = 0.455;

$A_f = 2.233\ \text{m}^2$;
$V = 13.88$ m/s;
ρ = density of air = 1.21 Kg/m^3;
Aerodynamic resistance = 0.5 × 1.21 × 0.455 × 2.233 × $(13.88)^2$ = 118.422 N.

18.7.3 Gradient Resistance

$$F_g = mg \sin \alpha \tag{18.6}$$

$\alpha = 13\%$;
Gradient resistance = 719 × 9.81 × sin (13%) = 859.158 N.

18.7.4 Road Load

$$ma_x = F_x - F_r - F_{\text{air}} - F_g \tag{18.7}$$

a_x is vehicle longitudinal acceleration in m/s$^{2;}$
F_x is the propelling force at wheels in N;
F_r is the rolling resistance;
F_{air} is the aerodynamic resistance;
F_g is the gradient resistance.
Propelling force at wheels = F_x

$$F_x = f_r mg \cos \alpha + \frac{1}{2} \rho C_d A_f (v)^2 + mg \sin \alpha + ma_x \tag{18.8}$$

18.7.5 Resistance Summary

Rolling resistance = 96.631 N.

Aerodynamic resistance = 118.422 N.

Gradient resistance = 859.158 N.

Acceleration resistance = 445.061 N.

For estimating the rated power of motor, rolling resistance, aerodynamic resistance, and acceleration resistance is accounted. While computing peak power, gradient resistance is also included.

$$P_{\text{rated}} = (96.631 + 118.422 + 445.061) \times 13.88 = 9.162\ \text{kW}$$

$$P_{\text{peak}} = (96.631 + 118.422 + 445.061 + 859.158) \times 13.88 = 21.085\ \text{kW}$$

Based on the tractive effort calculations, it is observed that the rated power is 9.162 kW and peak power is 21.085 kW. This power will vary according to the driving cycle considered. The motor selected should support the rated power and peak power required by the vehicle.

18.7.6 Motor Selection

Switched Reluctance Motor (SRM) has wide speed range and high torque density. It also has reasonable power density for small electric vehicle. SRM has different configurations of stator and rotor poles. For 15 kW rated power, 6/4 and 8/6 configuration was considered in this paper. The peak torque of 8/6 is low when compared with 6/4. Hence, when 8/6 SRM is employed in real driving conditions the peak torque may not be sufficient to propel the vehicle under stiff gradients. Therefore, SRM 6/4 configuration is considered in this paper. The specifications of SRM is given below(Maryniuk 2017):

- No. of poles on Stator = 6
- No. of poled on rotor = 4
- Rated power = 15 kW
- Peak power = 30 kW
- Torque = 110 Nm
- Voltage = 192 V
- Speed = 10,000 RPM.

The driving cycle considered in this paper is Indian Driving Cycle. It is depicted in the Fig. 18.3.

18.7.7 Gear Ratio Design

$$\omega_w = \frac{v_w}{r} \tag{18.9}$$

where ω_w is angular velocity of the wheel in rad/s;

v_w is vehicle velocity in m/s;

r is wheel radius in m.

The angular velocity of the wheel is calculated instantaneously for Indian driving cycle. Wheel torque is the product of tractive force and wheel radius. Hence, it is given by

$$T_w = FTR \times r \tag{18.10}$$

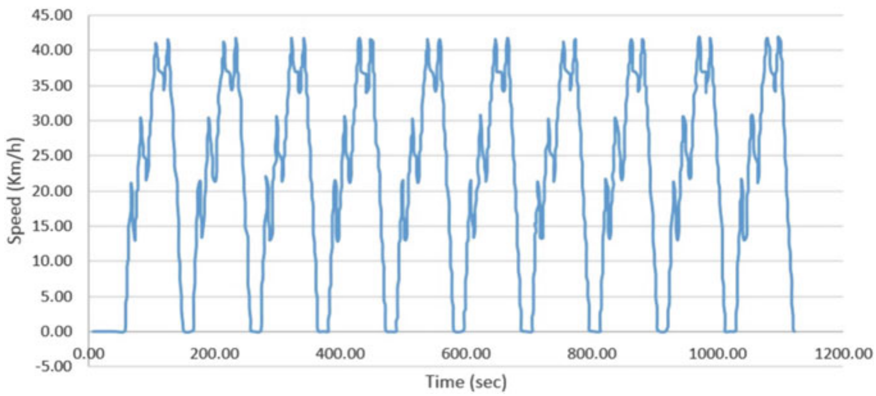

Fig. 18.3 Indian driving cycle for 2, 3 wheelers

where T_w is the wheel torque in Nm;

FTR is the tractive force in N;

r is the wheel radius in m.

Angular velocity of motor is given by

$$\omega_m = G \times \omega_w \tag{18.11}$$

where ω_m is the angular velocity of the motor in rad/s;

G is the gear ratio;

ω_w is the angular velocity of the wheel in rad/s.

Motor speed is calculated from the following equation:

$$N_m = \frac{\omega_m \times 60}{2\pi} \tag{18.12}$$

where N_m is the speed of the motor in rpm.

Motor torque is given by

$$T_m = \frac{\omega_w \times T_w}{0.98 \times \omega_m} \tag{18.13}$$

Here, the gear efficiency is assumed as 98% and

T_m is the motor torque in Nm.

Motor Power can be calculated by

$$P_m = T_m \times \omega_m \tag{18.14}$$

Here, P_m is the motor power in Watts.

For calculating the motor voltage, stroke angle and Psi peak are required. According the motor specifications, stroke angle is 0.5233 and Psi peak is 0.44.

Table 18.1 Comparison of motor system voltage

Voltage (V)	48	72	192
Gear ratio	1.25	1.9	5
Maximum constant gradient (degree)	5	5	5
Motor peak power on flat road (kW)	2.5	2.5	2.5
Motor peak power on gradient (kW)	9.6	9.6	9.6
Motor torque on flat road (Nm)	42	28	11
Motor torque on gradient (Nm)	110	110	110
Motor current on flat road (A)	50	33.54	12.35
Motor current on gradient (A)	127.48	127.48	127.48

Hence, the motor voltage is given by

$$V_m = \frac{\text{Psi peak} \times \omega_m}{\text{Stroke angle}} \tag{18.15}$$

Clearly, from Table 18.1, variation in motor system voltage doesn't affect the rated power and peak power consumed by the motor. If the system voltage is increased then in order to support the driving cycle, gear ratio have to be increased. Maximum constant gradient also doesn't depend on system voltage but it has direct relationship with motor torque and current. At level roads the scenario is different. The peak values of motor torque and current are same when the system voltage is varied. At lower voltages, increase in motor current increases the heat generation in the system. Hence, motor insulation should be given properly. Motor current and torque has a direct relationship between them. Even though motor is capable of providing high torque, increase in motor current increases the heat generation.

18.7.8 Effects on Battery Pack

As the motor voltage and battery voltage are same, placing cells in series for 48, 72, and 192 V system is applicable in small electric vehicle on both front and rear boot space available; 192 V is the maximum voltage possible for a small electric vehicle having width less than 1.5 m. Hence, the battery voltage also limited to 192 V. While connecting the cells in parallel, front boot supports up to 94.5 Ah, i.e., keeping three layers in the battery pack. In this system, the first layer consists of 40.4 Ah (15 cells in parallel), second layer contributes 32.4 Ah (12 cells in parallel), and third layer contributes 21.6 Ah (8 cells in parallel). The number of cells placed in parallel is getting reduced as no. of layers in the battery pack got increased. This is due to the phenomena of vehicle aerodynamics at the front.

At rear 216 Ah is possible with four layers of battery pack by keeping 20 cells per layer. Tata Tigor has 216 Ah battery pack. But keeping 216 Ah battery pack at the rear boot increases the battery weight as well as it affects the vehicle dynamics also. For retro-fitment purpose, keeping battery pack at the rear will change the drive configuration. Hence, rear battery pack is not recommended.

18.7.9 Weight Analysis for Battery Pack

In this analysis, the battery considered is LFP 3.6 V 2.7 Ah cylindrical cell. Motor voltage is varied and the projected battery weight is estimated is depicted in Table 18.2

For keeping battery pack at the front higher system, voltage is recommended to get a decent range. If the battery pack is placed at the rear boot, then lower system voltage is good otherwise the battery pack weight will increase and also weight distribution is affected. Indian electric cars have low system voltage but they offer a decent range through floor mounted battery pack. In retro-fitment, floor battery is not recommended as it disturbs the existing monocoque chassis structure.

18.8 Battery Pack Selection and Optimization for SEV

Fitting a battery pack in small electric vehicle which will cater a range of 200 km per charge is a challenging task considering the dimensions available for mounting the battery pack. In retro-fitment scenario, the battery pack can be mounted at the front end by taking care of vehicle aerodynamics and also the volume constraints possessed by the front hood. The battery pack can also be mounted in the rear where the free volume for fitting the battery pack is higher than the front hood. Focusing on the vehicle drivetrain, electric motors can perform efficiently and also it won't affect the drivetrain dynamics of the electric vehicle. By assuming all the challenges mentioned above, the battery pack can be optimized in such a way that it can fit various motor operating voltages, battery form factors, and high energy density cells. The motors considered for fitting in to SEV are BLDC, PMSM, SRM (8/6), and SRM

Table 18.2 Projected weight of battery pack for motor system voltage

Voltage (V)	48	72	192
Front capacity (Ah)	94.5	94.5	94.5
Front battery capacity (kWh)	4.536	6.804	18.144
Front weight (kg)	23.1	33	89.1
Rear capacity (Ah)	216	216	216
Rear battery capacity (kWh)	10.368	15.552	41.472
Rear weight (kg)	56	80	216

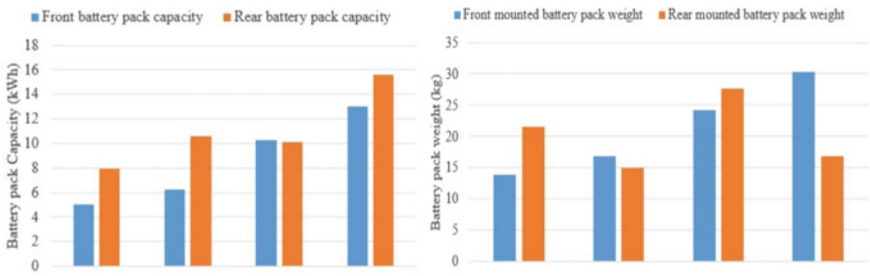

Fig. 18.4 **a** Battery pack capacity. **b** Battery pack weight

(6/4). The batteries considered in proposing the battery pack are lead–acid, Nickel–Metal Hydride, Lithium Polymer, Lithium–Sulfur, and Zinc-air. Based on the motor and battery pack selected, the optimized configuration for front- and rear-mounted battery packs which ensures a range of 200 km are given in the Fig. 18.4.

It is recommended to maintain the weight distribution of the SEV such that the center of gravity affects are negligible. The above figure shows the possible battery pack capacities which can be fitted in the SEV at front and rear ends. This also includes the projected weight of the SEV.

18.9 Retro-fitment Versus Purpose Built SEV

The benchmarked small passenger car has the following dimensions:

Length = 2800 mm,

Width = 1500 mm,

Height = 1600 mm.

Concept chassis is designed in solid works and it is exported to ANSYS for stress analysis. The concept chassis is depicted in Fig. 18.5

Volume available for battery mounting (L × B × H) = 2300 × 1300 × 200 mm.

For making the battery pack easily scalable, 12 V 35 Ah battery is considered.

The dimensions of the battery module are 175 × 104 × 165 mm and weight is 4.53 kg per module.

The maximum number of battery modules that can be mounted on the floor is 11 modules in series and 10 modules in parallel. Thus, the battery weight propels up to 500 kg on the floor. Here, the motor voltage is the key to designing scalable battery packs. For example, if the motor voltage is 72 V, then six batteries must be placed in series. Thus, by keeping ten modules in parallel, the battery rating reads 72 V 350 Ah and therefore the battery capacity reaches 25.2 kWh. The possibilities for a scalable battery pack are discussed below. Each battery module of different battery ratings is selected in such a way that it can be inserted in the floor space available. The battery modules considered in this paper are given in Table 18.3. Data for each

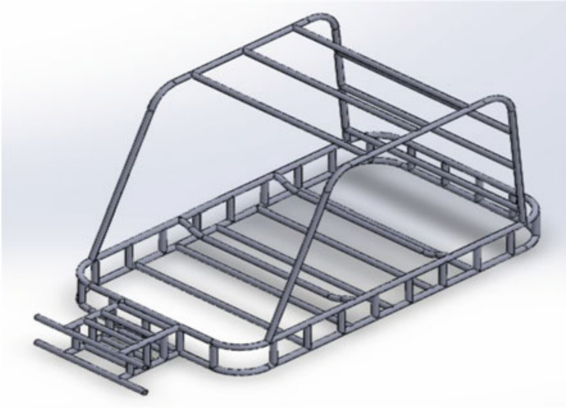

Fig. 18.5 Concept chassis for purpose built SEV

Table 18.3 Battery modules considered in this paper

Voltage (V)	12	24	48	72	96	192
Length (mm)	175	342	290	367.9	280	94.5
Width (mm)	165	205	210	183.9	200	18.144
Height (mm)	105	75	100	65.2	180	89.1
Capacity (Ah)	35	35	35	35	35	216
Weight (kg)	4.53	9	7.3	9.8	18	41.472
Battery shell	PVC	PVC	PVC	PVC	PVC	216

module is obtained from the website which is given after the reference section.

As discussed in Table 18.4, 35 Ah rating is kept constant in this paper because the battery pack benchmarked was Mahindra e2o (210 Ah). In the specifications page (Kept in Website, Reference section), 16 modules are used. Hence, the maximum length of the battery pack is obtained when 8 modules are kept parallel. Therefore, by keeping 8 modules of 35 Ah each, 210 Ah is obtained. Also, the various combinations of scaling the battery pack within the dimensional limits must be addressed. In Table 18.2 voltage scaling is done by keeping the 12 V battery module. This calculation is repeated for 24 V (shown in Table 18.5), 48 V (shown in Table 18.6), 72 V (shown in Table 18.7), and 96 V (shown in Table 18.8).

Table 18.4 Battery module having 12 V 35 Ah rating

Voltage (V)	48	72	96	120
Number of cells in series	4	6	8	10
Number of cells in parallel	6	6	6	6
Max. projected weight of battery pack (kg)	108.72	163.08	217.44	271.8
Max. projected battery capacity (kWh)	10.08	15.12	20.16	25.2

Table 18.5 Battery module having 24 V 35 Ah rating

Voltage (V)	48	72	96	120	144
Number of cells in series	2	3	4	5	6
Number of cells in parallel	6	6	6	6	6
Battery capacity for e2o (210 Ah)	10.8	15.12	20.16	25.2	30.24
Projected battery weight (kg)	108	162	216	270	324

Table 18.6 Battery module having 48 V 35 Ah rating

Voltage (V)	48	96	144	192	240	288	336
Number of cells in series	1	2	3	4	5	6	7
Number of cells in parallel	6	6	6	6	6	6	6
Battery capacity for e2o (210 Ah)	10.08	20.16	30.24	40.32	50.4	60.48	70.56
Projected battery weight for e2o (kg)	43.8	87.6	131.4	175.2	219	262.8	306.6

Table 18.7 Battery module having 72 V 35 Ah rating

Voltage (V)	72	144	216	288	360	432
Number of cells in series	1	2	3	4	5	6
Number of cells in parallel	6	6	6	6	6	6
Battery capacity for e2o (210 Ah)	15.12	30.24	45.36	60.48	75.6	90.72
Projected battery weight for e2o (kg)	58.8	117.6	176.4	235.2	294	352.8

Table 18.8 Battery module having 96 V 35 Ah rating

Voltage (V)	96	192	288	384	480	576	672	768
Number of cells in series	1	2	3	4	5	6	7	8
Number of cells in parallel	6	6	6	6	6	6	6	6
Battery capacity for e2o (210 Ah)	20.16	40.32	60.48	80.64	100.8	120.96	141.12	161.28
Projected battery weight for e2o (kg)	108	216	324	432	540	648	756	864

Weight-based optimization is carried out from the possible combinations of the battery pack with scaled voltage. The threshold weight of the battery pack is kept at 200 kg and tolerance is kept as ±50 kg. The various battery combinations with scaled voltage are shown in Tables 18.9 and 18.10.

While selecting the chassis materials, the factor of safety is kept at 5. Hence, the designed chassis can withstand 1000 kg of battery pack before failure. Initially, the maximum possible battery voltage is fixed from the calculations shown above. It is followed by the chassis materials considered in ANSYS is given in Table 18.11.

Table 18.9 Battery optimization for 200 + 50 kg

Voltage (V)	12	24	48	72	96
Individual module capacity (Ah)	35	35	35	35	35
Max battery pack voltage (V)	96	96	240	288	192
Battery capacity (Ah)	210	210	210	210	210
Projected battery capacity (kWh)	20.16	20.16	50.4	60.48	40.32
Projected battery weight (kg)	217.44	216	219	235.2	216

Table 18.10 Battery optimization for 200 − 50 kg

Voltage (V)	12	24	48	72
Individual module capacity (Ah)	35	35	35	35
Max battery pack voltage (V)	72	72	192	216
Battery capacity (Ah)	210	210	210	210
Projected battery capacity (kWh)	15.12	15.12	40.32	45.36
Projected battery weight (kg)	163.08	162	175.2	176.4

Here, the 96 V battery is not considered because the weight difference is too large based on the given boundary conditions. From the upper boundary, it is clear that the battery voltage scaled from 12 to 288 V and for lower boundary, the battery voltage scaled from 12 to 216 V. This voltage projection is applicable for the dimensions considered in designing the SEV. The proposed battery pack can be scaled for sedans, SUV's, etc., where the length and width of the volume available for mounting can be improved based on their dimensions. The materials considered for structural analysis is given in Table 18.11 where the upper and lower boundaries of battery pack is given in Tables 18.12 and 18.13.

18.9.1 Boundary Conditions

Fixed support = Bottom boundary of the chassis.

Force = 10,000 N (on the support bars for mounting the battery pack.

Output = Total deformation (mm) and Equivalent stress (Mpa).

The weight of the chassis obtained from ANSYS 2019 R1 is shown in Fig. 18.6. The results obtained from ANSYS while substituting the boundary conditions are shown in Fig. 18.7 and Fig. 18.8. Deformation and structural analysis of Al 6082 T6 and Mg alloy were shown in Figs. 18.9, 18.10, 18.11 and 18.12, respectively.

Based on the structural analysis in ANSYS, the weight of the chassis is taken. Before doing the weight distribution, the assumptions considered in this analysis are given below.

- BIW weight (W_b) = 100 kg

Table 18.11 Materials considered for chassis in ANSYS

Material	Steel	Alloy steel	Al 6082 T6	AISI 9000	Mg Alloy	Al Alloy	Al 6063 T4	Al 6061 T4	AISI 1018
Density (kg/mm^3)	7861	7700	2449.34	7076.40	1800	2770	2690	2700	8000
Youngs modulus (MPa)	205	210	72	207	45	71	69	69	210
Poisson ratio	0.29	0.28	0.33	0.29	0.35	0.33	0.33	0.33	0.3
Tensile strength (MPa)	772.56	723	270	850	540	648	80	130	634

Table 18.12 Upper boundaries of the optimized battery pack

Chassis	12 V	24 V	48 V	72 V	96 V
Steel	488.05	486.61	489.61	505.81	486.61
Alloy steel	485.94	484.5	487.5	503.7	484.5
Al 6082 T6	411.954	410.514	413.514	429.714	410.514
AISI 9000	477.152	475.712	478.712	494.912	475.712
Mg alloy	403.07	401.63	404.63	420.83	401.63
Al 6063 T4	415.344	413.904	416.904	433.104	413.904
Al 6061 T4	415.845	414.405	417.405	433.605	414.405
AISI 1018	490.17	488.73	491.73	507.93	488.73

Table 18.13 Lower boundaries of the optimized battery pack

Chassis	12 V	24 V	48 V	72 V
Steel	433.69	432.61	445.81	447.01
Alloy steel	431.58	430.5	443.7	444.9
Al 6082 T6	357.94	356.514	369.714	370.914
AISI 9000	422.792	421.712	434.912	436.112
Mg alloy	348.71	347.63	360.83	362.03
Al 6063 T4	360.984	359.904	373.104	373.304
Al 6061 T4	361.485	360.405	373.605	374.805
AISI 1018	435.81	434.73	447.93	449.13

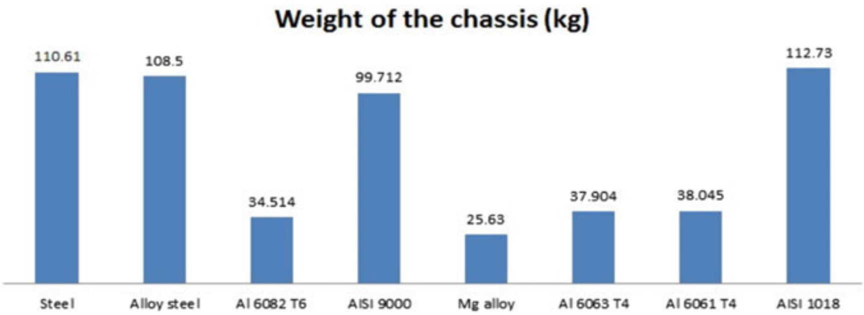

Fig. 18.6 Chassis weight comparison for purpose-built SEV

- Motor weight (W_m) = 40 kg
- Miscellaneous (W_M) = 10 kg
- Transmission (W_t) = 10 kg.

$$W_{\text{Body}} = W_b + W_m + W_M + W_t \tag{18.16}$$

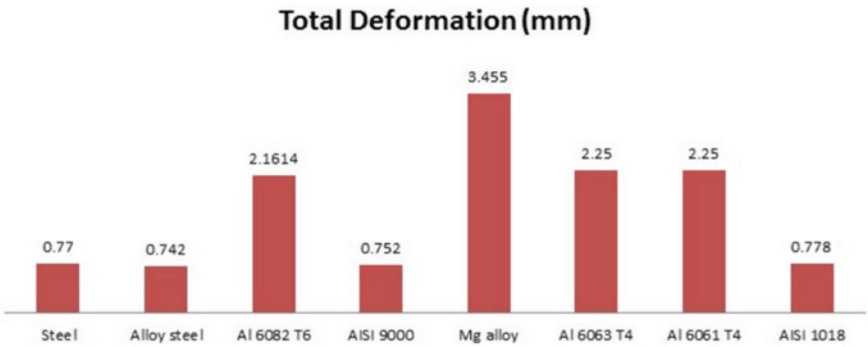

Fig. 18.7 Total deformation applicable to various chassis materials for SEV

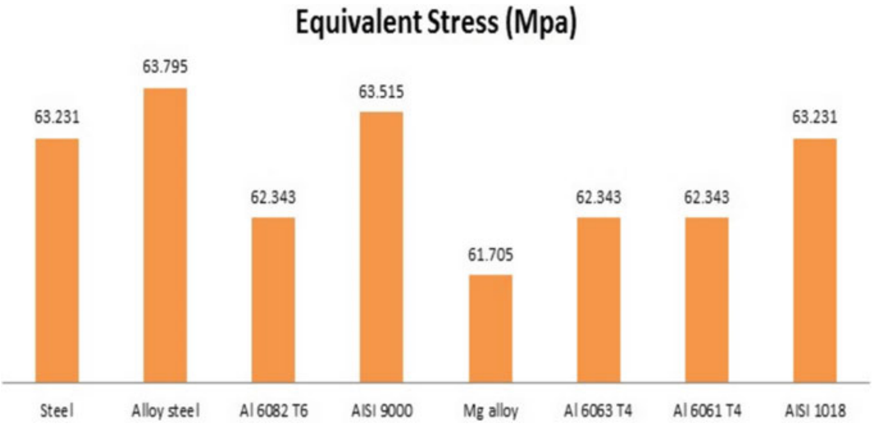

Fig. 18.8 Equivalent Stress applicable to various chassis materials for SEV

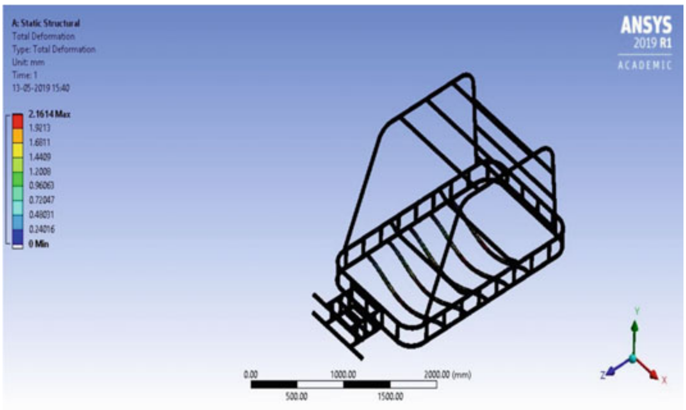

Fig. 18.9 Total deformation of the concept chassis applicable to SEV

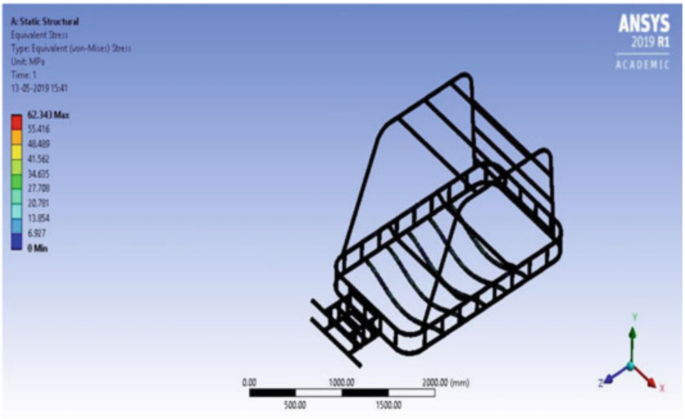

Fig. 18.10 Equivalent stress of the concept chassis applicable to SEV

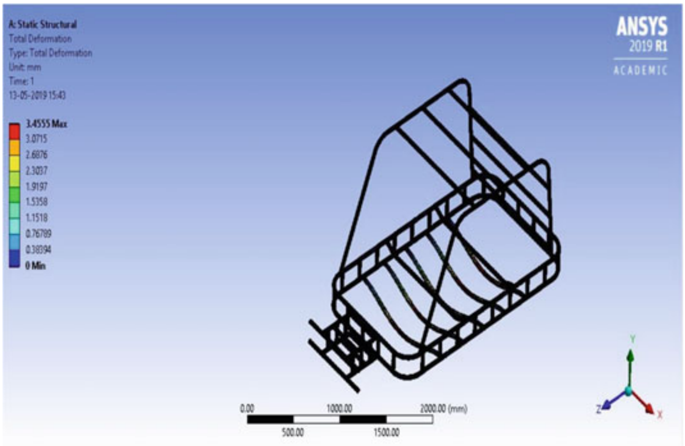

Fig. 18.11 Total deformation of the concept chassis applicable to SEV

where W_b is the BIW weight of the electric vehicle (kg).

W_m is the motor weight (kg).

W_M is the miscellaneous weight (kg).

W_t is the transmission weight (kg).

Hence, the weight to be kept constant is 160 kg. In addition to this, optimized battery pack weight and chassis weight are added together.

$$W_k = W_{\text{Body}} + W_{\text{Chassis}} + W_{\text{battery pack}} \tag{18.17}$$

where W_K is the curb weight of the electric vehicle.

W_{Body} is the body weight (kg).

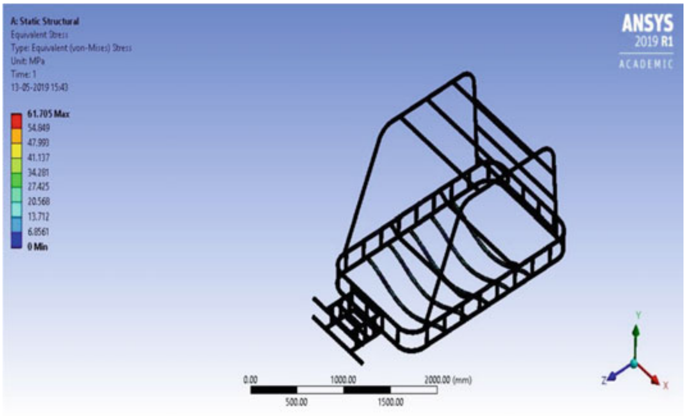

Fig. 18.12 Equivalent stress of the concept chassis applicable to SEV

W_{chassis} is the chassis weight (kg).

$W_{\text{battery pack}}$ is the battery pack weight (kg).

Based on the above design of experiments for the upper and lower boundary, the chassis should be made up of Al alloys and magnesium alloy. The lowest possible curb weight of the chassis for the upper boundary of the battery pack is 401.63 kg for magnesium alloy and for aluminum alloys the curb weight varies from 410 to 435 kg. When the lower boundary of the battery pack is considered, the lowest possible curb weight of chassis is 347.63 kg and for aluminum alloys, it varies from 356 to 375 kg. For SEV upper boundary of the battery pack capacity is quite high. Even though space is available at the floor for mounting the battery pack, a battery capacity of more than 20 kWh is not recommended. Hence, even in lower boundary also inserting 48 and 72 V modules are not recommended. The possible battery capacity which meets the requirements of SEV is 15.12 kWh from the lower boundary of the battery pack. This battery capacity is at par with Mahindra e2o, Tata Tigor, MAHLE Mahle Efficient Energy Transport (MEET) vehicles. Battery pack weight varies from 162 to 163 kg which is well inside the limit of 200 kg. Therefore, the lowest possible curb weight of the proposed SEV is 347.63 kg. Adding the passenger weight of 300 kg (4 passengers, each 75 kg) and payload of 20 kg, the gross weight of the proposed SEV is 667.63 kg. The curb weight of the IC engine variant is 451 kg. Hence, using Mg alloy chassis 22.93% weight reduction (curb weight) is possible. For aluminum alloys, it works out to be 16 to 21%.

18.10 Discussion on Road Load Coefficients

The SEV proposed in this paper will have the following specifications shown in Table 18.14.

Table 18.14 Specifications of SEV

Kerb weight (kg)	450
Pay load (kg)	20
Gross Vehicle Weight (kg)	750
Motor power (kW)	15 (SRM, 6/4)
Torque (Nm)	110
Gear ratio	6.6:1
Maximum speed (km/h)	80
Gradient	15° at 40 km/h
Battery	192 V, 86.4 Ah (LFP)

The road load coefficients obtained from previous literature for small cars are given below. The force experienced by the vehicle during coasting down test is given by

$$F = A + Bv + Cv^2 \tag{18.18}$$

where F is the Road load force in N.

A, B & C are the road load coefficients.

v is the vehicle velocity in m/s.

Then the power consumed by the electric vehicle in coasting is given by

$$P = F \times v \tag{18.19}$$

where P is the power consumed in watts.

F is the Road load force in N.

v is the vehicle velocity in m/s.

The energy stored in the battery pack is exhausted after a certain amount of time say the operation of the electric vehicle. The time can be calculated by

$$t = \frac{\text{Battery Capacity}(kWh)}{P(kW)} \tag{18.20}$$

where t is the time taken by the vehicle to exhaust full of its energy in hours.

Distance traveled by the electric vehicle is estimated by

$$D = v \times t \tag{18.21}$$

where D is the distance traveled by the electric vehicle in km.

v is the vehicle velocity in m/s.

t is the time taken by the electric vehicle to exhaust its full energy in seconds.

The road load coefficients vary according to the vehicles tested in the chassis dynamometer. The values given by the EU, SAE, and Korres et al. are given in Table

Table 18.15 Road load coefficients

Coefficients	EU	SAE	Korres et al.
A	122.2	120.4	169.6
B	−0.443	−0.207	5.12
C	0.442	0.436	0.2869

18.15. Tests were conducted on a small electric car whose gross vehicle weight ranging from 750 to 950 kg. The proposed SEV falls in the bracket and hence the road load coefficients are compared in range estimation. The vehicle considered by Korres et al. has a curb weight of 831 kg, a maximum speed of 85 km/h and a range of 150 km. The range obtained when substituting the Korres et al., EU, and SAE values of road load coefficients in Eqs. 18.1, 18.2, and 18.5–18.8 is shown in Figs. 18.13, 18.14 and 18.15, respectively.

The distance covered by the electric vehicle designed by Korres et al. is depicted in the figure. It is observed that a 200 km range is possible only when the vehicle speed

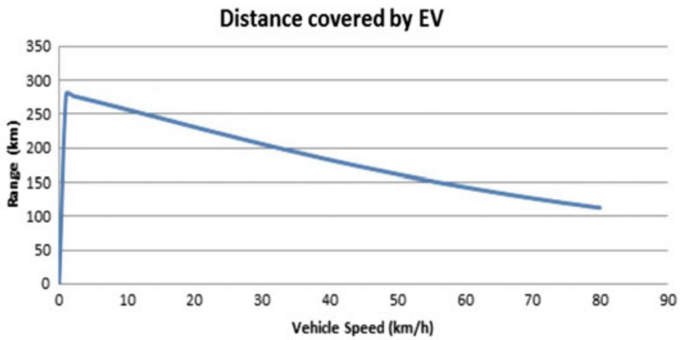

Fig. 18.13 Distance covered by the SEV under various speeds

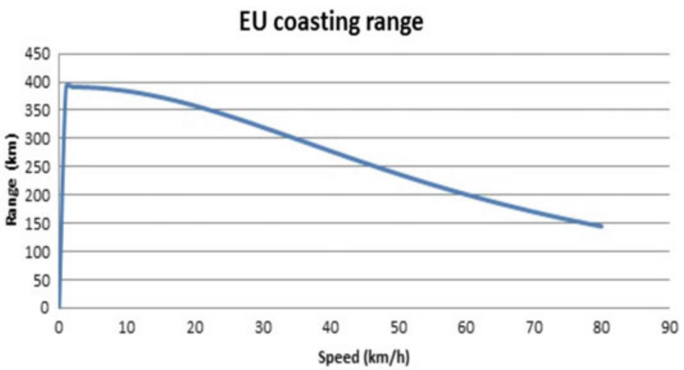

Fig. 18.14 European Union coasting range applicable to SEV

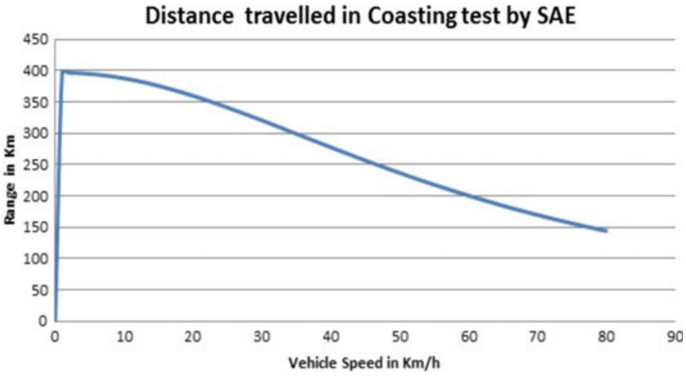

Fig. 18.15 Distance traveled in coasting test by SAE applicable to SEV

is between 30 and 35 km/h. Urban driving requires such speed ranges, especially in traffic conditions. While cruising the vehicle above 60 km/h the range drops to less than 150 km which seems to be realistic considering the battery pack provided for Mahindra e2o. The range provided by the manufacturer is 140 km for a 15-kWh battery pack. Generally, the usable energy capacity is always less than battery capacity. Assuming the usable battery capacity is 80% of total battery capacity, the usable capacity of the SEV proposed is 13.264 kWh, whereas, for Mahindra e2o, it is 12 kWh. The specific energy consumption for SEV when moving at speed of 30–35 km/h is 15.078 km/kWh and for e2o it is 11.667 km/kWh.

Euro 5 gasoline car is tested in chassis dynamometer and the coast down data for the same is given in Table 18.16.

Sample 5 is a small passenger hatchback gasoline engine car that meets Euro 5 Norms. Though the curb weight is higher than 1000 kg the road load coefficient values particularly the realistic one resembles the values declared by EU and SAE. The only change in value is the B coefficient which directly influences rolling resistance and aerodynamic resistance of the vehicle. A and C values are almost in the range when compared with the EU and SAE. From Fig. 18.16, a range of 200 km can be attained if the speed of the vehicle is in the range of 50–60 km/h (or) at an average speed of 55 km/h. This scenario is valid for a Realistic case where the actual road load forces will act on the vehicle. If the least squares fit method is implemented to estimate the coefficients after the completion of the coast down test, the average speed should be 60 km/h to obtain a 200 km range. Generally, the user ends up with 1 equation and three unknowns, therefore, the least squares fit is implemented to get the solution.

Table 18.16 Hatchback A segment coast down data

Sample 5	Type approval	Realistic	Least squares fit
A	86	123	114
B	0.612	1.008	0.3861
C	0.41472	0.41472	0.0281

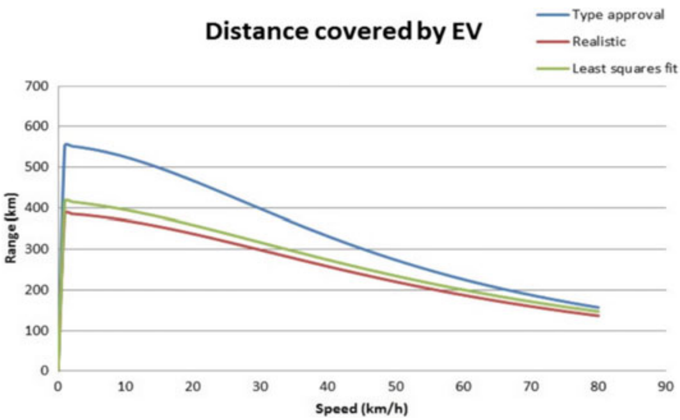

Fig. 18.16 Comparative distance covered by the proposed SEV under various coast down data

For getting type approval, the vehicle should be tested in ideal conditions, i.e., the vehicle will not experience the same in real driving conditions. In this test, the vehicle speed can reach up to 70 km/h for a range of 200 km. Based on the three cases for a sample, it is observed that maximum speed should be 55–70 km/h. This makes sense that the proposed SEV has maximum speed of 80 km/h will get a range of 200 km provided the weight of the SEV should be less than weight of Sample 5 and weight in the case of Korres et al. The curb weight of various models considered in this paper is shown in Fig. 18.16.

18.10.1 Model Validation

Here, the concept of the coast down mathematics empirical relationships was considered. The empirical relationships have a close correlation with vehicle dynamics. The expression of the vehicle deceleration during coast-down can be presented as a final function of speed is given by

$$\frac{\left[mg(f_0 + f_1 v)\cos\alpha + mg\sin\alpha + \frac{1}{2}\rho C_d A V^2 + Rf_0 + Rf_1 v\right]}{m_{ap}} = A + Bv + Cv^2 \tag{18.22}$$

where A $= \frac{\left[mg(f_0\cos\alpha + \sin\alpha) + \frac{1}{2}\rho C_d A V^2 + Rf_0\right]}{m_{ap}}$.

B $= \frac{\left[mg(f_0\cos\alpha) + \frac{1}{2}\rho C_d A V + Rf_1\right]}{m_{ap}}$.

C $= \frac{\left[\frac{1}{2}\rho C_d A\right]}{m_{ap}}$

Table 18.17 Braking results

Speed (km/h)	Distance (m)	Total stopping distance (m)	Kinetic energy (J)
80	35.99	53	177530.864
70	27.55	42	135922.067
60	20.24	32	99861.111
50	14.05	24	69347.993
40	8.99	17	44382.716
30	5.06	11	24965.277
20	2.24	6	11095.679
10	0.56	2	2773.919
0	0	0	0

$$m_{ap} = m \times \delta \tag{18.23}$$

$\delta = 1.03$ to 1.04
R_{f0} is the drive train resistance at low speeds.
R_{f1} is the increasing rate with the speed of resistance v.
$f_0 = 0.0076.$
$f_1 = 0.2$
$\alpha = 0°$ for flat roads.

While braking the vehicle, the kinetic energy at the wheels can be stored to the battery pack via regenerative braking concept. The braking distance of the vehicle moving at different speeds is given in Table 18.17.

After that, the power absorbed in the braking is estimated and the range calculated through the braking concept is depicted below. Referring to Fig. 18.17, the maximum speed range should be between 45 and 50 km/h during braking.

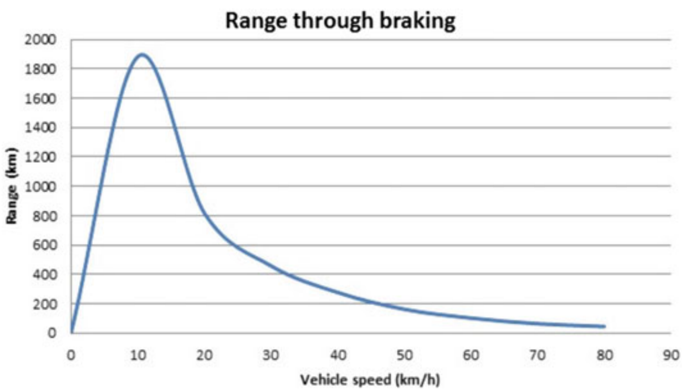

Fig. 18.17 Braking energy of the proposed SEV

18.11 Performance Analysis for SEV

Based on SEV parameters, the peak power and nominal power required by the motor is calculated from vehicle forces which is shown in Fig. 18.18.

The rated and peak power are computed at a speed of 50 km/h in the calculation. The maximum speed of the quadricycle is 70 km/h (Wismans et al. 2011). Referring to Fig. 18.18, the rated power is around 12 kW and the peak power is around 27 kW. Considering the maximum losses as 2 kW (Patel and Kumar 2017), the rated power should be 15 kW and the peak power should be 30 kW. Hence, through suitable gear reduction methods, 15 kW rated SRM is selected. The design of switched reluctance motor of 6/4 configuration is carried out according to the procedure (Patel and Kumar 2017; Tsirogiannis et al. 2019).

18.11.1 Specifications of Switched Reluctance Motor 15 kW (Patel and Kumar 2017)

Outer diameter of stator = 220 mm
Outer diameter of rotor = 116 mm
Stator pole width = 33 mm
Stator pole height = 17 mm
Rotor pole width = 33 mm
Rotor pole height = 16 mm
Shaft = 20 mm
Stator = 24 kg
Rotor = 9 kg
Accessories = 5 kg
Total weight of motor = 38 kg
Power output = 15 kW including losses

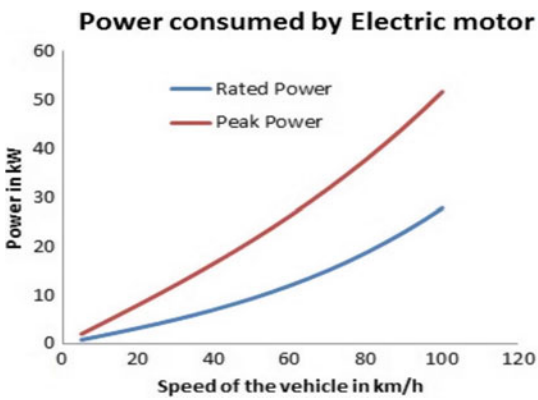

Fig. 18.18 Power consumed by SRM 6/4 for the proposed SEV

Speed = 1500 rpm
Torque = 111 Nm (calculated)
Torque = 100 Nm (expected after ripple losses).

18.11.2 Motor Losses

The losses are Copper loss, Iron loss, and windage loss.

$$q = \frac{4\sqrt{3T}}{BK\pi D^2 L} \tag{18.24}$$

where T is the output torque from the motor in Nm B is the magnetic flux density in Wb/m^2.

K is the constant which defines the saturation factor of the motor. For fully saturated condition $K = 0.75$.

D is the outer diameter of the stator in m.

L is the length of the stator (or) stack length in m.

q is the electric loading.

$$I_{\text{peak}} = \frac{q\pi D_i}{6N_{ph}} \tag{18.25}$$

where D_i is the inner diameter of the rotor in m.

N_{ph} is the number of turns per phase.

I_{peak} is the stator peak current in A.

$$I_{rms} = \frac{I_{peak}}{\sqrt{m}} \tag{18.26}$$

where m is the number of phases (usually for SRM m = Stator poles/2).

I_{rms} is the rms current in A.

For estimating the Copper loss (P_{cu}).

$$P_{\text{cu}} = 3I_{\text{rms}}^2 R \tag{18.27}$$

where P_{cu} is the copper loss in W.

R is the internal resistance in the motor in ohms.

The iron loss and winding loss is kept constant as 100 W and 5 W, respectively.

18.12 Performance Parametric Evaluation for SEV

The SEV's are intended to match the performance of urban mobility requirements. However, in particular, the Indian Driving Cycle for three-wheelers is considered with constant gradient of 10.2° and 15°. Since, the benchmarked vehicle belongs to quadricycle, the three-wheeler driving cycle justifies the power requirements regarding lower limits. Also the simulation is being performed with NEDC for benchmarking the upper limit. Recent trends show that Switched Reluctance Motor with 6/4 configuration provides 110 Nm torque at a peak power of 30 kW justifies Indian Driving Cycle with 15° gradient and also NEDC with maximum speed of 100 km/h (till phase 2 and some short range in phase 3).

Referring to the Fig. 18.19, the proposed SEV will match with IDC with top speed being 42 km/h. Urban mobility is altogether a different scenario where start and stop become the mandatory. 580 kg is the kerb weight of the vehicle benchmarked from 22 (Tanik and Parlaktaş 2015). To overcome range anxiety, the vehicle weight along with the battery capacity needs to be refined in such a way that the performance of the vehicle remains unaltered. Modern SOC estimation algorithms do prefer the datasets associated with vehicle testing parameters. Real-world test data is extremely important to benchmark a vehicle for its subsequent steps on electrification and testing protocols (Sankaran et al. 2020; Scheubner et al. 2019; Mashhoodi and Blij 2021; Petersen et al. 2019). The specifications of the proposed SEV for retro-fitment purpose is shown in Table 18.18.

The simulations performed in MATLAB/Simulink and mathematical formula from CarlosGertz et al. (2014) is used for validation. The distance traveled by the PHEV in full electric mode is given by

$$S_{\mathrm{AER}} = Zkn_{\mathrm{CD}} \tag{18.28}$$

where S_{AER} is the distance traveled by the Electric vehicle in miles.

Z is the battery swing window (Actually it resembles initial SOC of the battery, $Z = 0.8$).

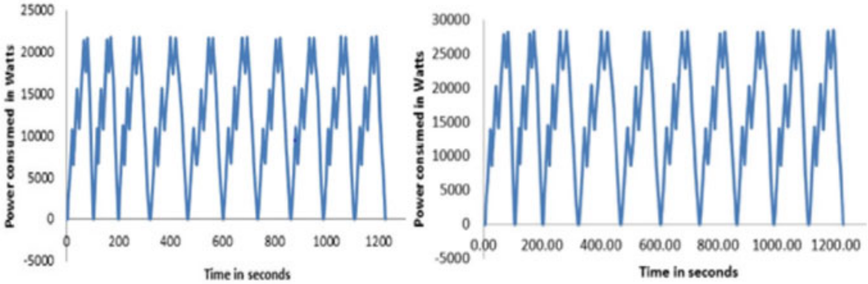

Fig. 18.19 Power consumption of the proposed SEV for a gradient of 10.2° (left) and 15° (right)

Table 18.18 Specifications of proposed SEV

Electric motor	Switched reluctance motor
Motor rated output power (kW)	15
Motor peak output power (kW)	30
Motor peak torque (Nm)	110
Battery pack output voltage	192
Battery current capacity	86.4
Battery chemistry	LFP
Theoretical battery pack capacity (kWh)	16.58
Usable battery pack capacity (kWh)	13.264
Top speed (km/h)	50
Final drive reduction ratio	8.8:1
Wheel diameter (mm)	493
Expected range (km)	200
Motor weight (kg)	50
Battery weight (kg)	80
Miscellaneous (kg)	40
Payload (kg)	20
Expected weight of BIW, seats, Instrumentation panel, wheels (kg)	492

k is the total battery capacity in kWh.

n_{CD} is the fuel economy from simulation (miles/kWh) (Fig. 18.20).

Powertrain performance parameters were estimated in Simulink simulations. Driving cycles are altered to analyze the motor and battery pack performance. Figure 18.21 shows the sample output of EV reference application in Simulink.

Usually, city-type driving cycle caters a range over 200 km. Artemis motorway 150 and HWFET were also simulated by keeping the boundary conditions constant. Driving conditions are really important in electric vehicle range prediction. The

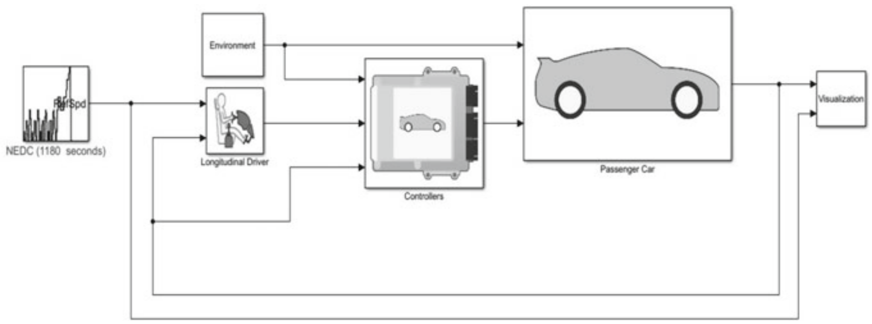

Fig. 18.20 Electric vehicle reference application from MATLAB/Simulink

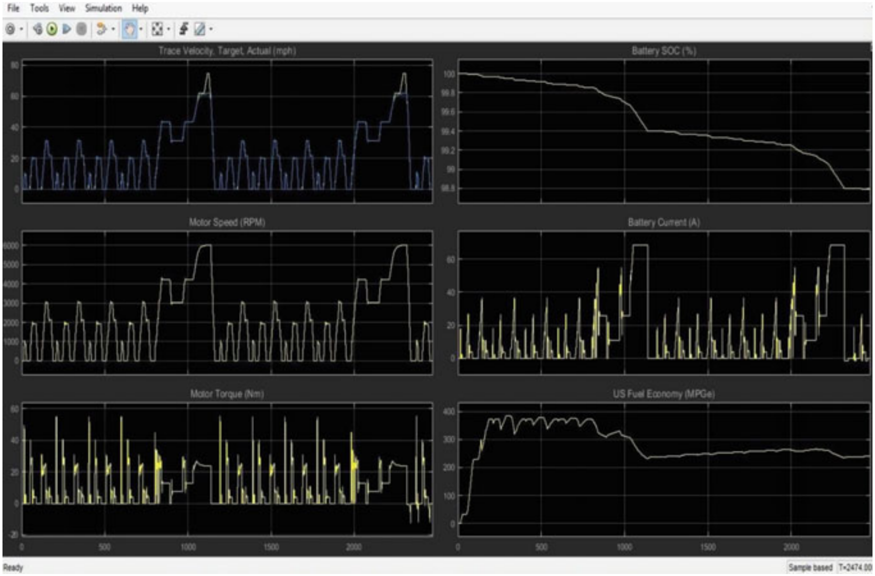

Fig. 18.21 Summary of results for the performance simulation of SEV

retro-fitted SEV is compared with MIA electric car and its specifications are shown in Table 18.19.

18.13 Conclusion

SEV requires a minimum range of 200 km in such a way that it can potentially act as an alternative to taxi's/cabs in urban mobility. The advantage of SEV can be of lower vehicle size as compared to a car. Since the SEV considered in this research is benchmarked from a quadricycle, the power to weight ratio can be quantified as 23.96 kg/kW. An SEV to be classified under WLTC cycle 1 requires minimum of 22 kg/kW and it should be able to sustain the speeds of 65 km/hr. Preferring SRM over BLDC, PMSM propels the proposed SEV to a maximum speed close to 100 km/hr. In retro-fitment scenario, fitting the battery pack in the front and motor at the rear, augurs well for maintaining stability in drivetrain dynamics and also the effective vehicle center of gravity. Lithium-ion cylindrical cells are preferred for retro-fitment case. If the SEV is designed from scratch, it can be able to accommodate the battery pack on floor. Pouch type of lithium cells can be fitted effectively on the floor which is capable of holding the battery pack weight of 200 kg in purpose built design of SEV. Also the reports on stress analysis states that aluminum alloys can be used as chassis materials for roll cage-type structure. Based on comparative study, the retro-fitted SEV performs close to the top SEV's benchmarked across the globe. In terms

Table 18.19 Comparison of proposed vehicle with MIA electric

Properties	MIA electric (Norrby 2012)	Proposed vehicle
Dimensions (mm)	3190 × 1640 × 1550	2752 × 1312 × 1652
Wheel base (mm)	1960	1925
Turning radius (m)	4.3	3.47
Number of seats	4	4
Battery type	LFP	NCA
Nominal voltage (V)	76.8	192
Battery energy (kWh)	12.3	17.23
Battery mass (kg)	145	75
Kerb weight (kg)	850	560
Gross weight (kg)	1200	900
Motor type	Asynchronous	Asynchronous
Motor	Induction	Switched reluctance
Motor power (kW)	10	9.38
Motor peak power (kW)	18	21.3
Motor torque (Nm)	65	110
Gear box	Single speed 8:1	Single speed 6.6:1
Body structure	Cold rolled steel closed sections And sheet steel joined by welding	Advanced high strength steels
NEDC vehicle range (km)	125	198.42
Specific energy consumption (Wh/km)	96	86.88
Maximum speed (km/h)	100	96.54

of performance, NEDC driving cycle up till phase 2 is applicable which guarantees a minimum speed of 80 km/hr to sustain in NEDC. In Transmission part, SRM motor having 6/4 configuration has supply voltage of 192 V and hence considering the retro-fitment and purpose built scenario, lithium-ion cylindrical cells with NCA chemistry is preferred for 200 km range.

Retro-fitted vehicles can be preferred when the vehicle population is high before vehicle electrification. However, the existing vehicles do have space constraints to be addressed by the retro-fitment kit supplier or an organization to come up with potential solutions which makes sense to vehicle electrification. The purpose-built vehicles make sense where the scalable battery packs are given the preference considering range anxiety and better control over weight distribution along with modifications in the chassis. Hence, the purpose-built vehicles can be preferred when there is a new product development which has to be started from scratch. Based on the analysis carried out in this chapter, the SEV has plenty of benefits to the urban mobility users when it is nurtured properly to cater the demands from shared mobility, vehicle electrification plans from the government and achieving the sustainability development goals. From the scalable battery pack configuration, the capability of V2G can be addressed for supporting the electricity grid when the vehicle is idle. Overall, the growth of SEV can redefine the electric mobility in all facets towards improvement.

References

Arora S, Kapoor A, Shen W (2018) Application of robust design methodology to battery packs for electric vehicles: identification of critical technical requirements for modular architecture. Batteries 30:4. https://doi.org/10.3390/batteries4030030

Arun D, Paleshwar DV, Sainath K (2019) Electric vehicle chassis design and structural analysis by using CAD and CAE techniques. Int J Res Eng Sci Manage 2(4):323–327

Barlow TJ, Latham S, Mccrae IS, Boulter PG (2009) A reference book of driving cycles for use in the measurement of road vehicle emissions. Published project report 354, TRL Limited

Barta D, Mruzek M, Labuda R, Skrucany T, Gardynski L (2018) Possibility of increasing vehicle energy balance using coasting. Adv Sci Technol Res J 12(1):228–235. https://doi.org/10.12913/22998624/86215

Berjoza D, Jurgena I (2017) Effects of change in the weight of electric vehicles on their performance characteristics. Agronomy Res 15(Special Issue 1):952–963

Bobbaa S, Mathieuxa F, Ardentea F, Blenginia GA, Cusenzac MA, Podiasd A, Pfrangd A (2018) Life cycle assessment of repurposed electric vehicle batteries: an adapted method based on modelling energy flows. J Energy Storage 19:213–225

Cano ZP, Banham D, Ye S, Hintennach A, Lu J, Fowler M, Chen Z (2018) Batteries and fuel cells for emerging electric vehicle markets. Nat Energy, Review Article. https://doi.org/10.1038/s41560-018-0108-1

CarlosGertz L, Cervieri A, AiresRodrigues AF, De Albuquerque L (2014) Chassis design for electric car prototype. SAE technical paper 2014-36-0215

Chander A, Kumar M, Nambiar S, Zaveri H (2018) Design and study of transmission system for electric vehicles. Int J Eng Sci Comput 8(3):16512–16514

Ciuffo B, Fontaras G, Id SS, Garcia MO (2017) Impact of different driving cycles and operating conditions on CO_2 emissions and energy management strategies of a Euro-6 hybrid electric vehicle. Energies 10:1590. https://doi.org/10.3390/en10101590

Determination and Use of Road Load Force and Dynamometer Settings (2015) United States Environmental Protection Agency National Vehicle and Fuel Emissions Laboratory 2565 Plymouth Road Ann Arbor, Michigan, Feb. CD-15-04 (LDV/LDT/ICI/LIMO)

Dinger A, Martin R, Mosquet X, Rabl M, Rizoulis D, Russo M, Sticher G (2010) Focus batteries for electric cars, challenges, opportunities and the outlook to 2020. Boston Consulting Group.

Driving into 2025: The future of electric vehicles. https://www.ngevehicles.com/ev-technical/driving-into-2025-the-future-of-electric-vehicles.html. Last accessed 11 June 2019

Dubarry M, Baure G, Pastor-fernández C, Fai T, Widanage WD, Marco J (2018) Battery energy storage system modelling: a combined comprehensive approach. J Energy Storage 21:172–185

Faid S (2015) A highly efficient two speed transmission for electric vehicles. EVS 28 KINTEX, Korea, May 3–6

Gis W, Żół towski A, Bocheńska A (2012) Testing of the electric vehicle in driving cycles. J KONES Powertrain Transport 19(4)

Highway code stopping distances. https://www.highwaycodeuk.co.uk/answers/what-is-the-stopping-and-braking-distance-of-a-car. Last accessed 8 Aug 19

Hofman I, Sergeant P, Van den Bossche A, Koroglu S, Kesler S (2016) Optimal design and implementation of a drivetrain for an ultra-light electric vehicle. Int J Vehicle Design 72(3):262–283

Humphries K, Morozov A (2016) A comparison of vehicle simulation software and dynamometer results for battery electric vehicles. In: Proceedings of The Canadian Society for Mechanical Engineering International Congress 2016, CSME International Congress, June 26–29, Kelowna, BC, Canada

Implementation of SAE J1634 (1997) Electric vehicle energy consumption and range test procedure. ETA–TP 003, 1–24

Isobe F, Itakura Y, Osumi Y, Li G (2011) One motor type electric vehicle drive system. Ntn Tech Rev 79:33–41

Kachapornkul S, Jitkreeyarn P, Somsiri P, Tungpimolrut K (2007) A design of 15 kW switched reluctance motor for electric vehicle applications. In: Proceeding of international conference on electrical machines and systems 2007, Oct. 8~11, Seoul, Korea, pp 1690–1693

Kadijk G, Ligterink N (2012) Road load determination of passenger cars. TNO report, TNO 2012 R10237, October 2012

Karabasoglu O, Michalek J (2013) Influence of driving patterns on life cycle cost and emissions of hybrid and plug-inn electric vehicle powertrains. Energy Policy. https://doi.org/10.1016/j.enpol.2013.03.047

Koumartzakis G, Spanoudakis P, Tsourveloudis NC (2017) Design and development of a prototype electric vehicle's chassis. In: 7th BETA CAE international conference

Kristyadi T, Putra A, Santika T, Hartawan L, Trinaldo (2017) Stress analysis of a cross over electric car chassis. IOSR J Mech Civil Eng (IOSR-JMCE) 14(5 Ver. I):13–28. e-ISSN: 2278–1684, p-ISSN: 2320–334X

Kühlwein J (2016) Driving resistances of light-duty vehicles in Europe: present situation, trends, and scenarios for 2025. White paper, ICCT, December

Lampic G, Gotovac G, Geaney H, O'Dwyer C (2016) Comparing the suitability of Lithium ion, Lithium Sulfur and Lithium air batteries for current and future vehicular applications. arXiv:1606.06347

Lesemann M, Stein J, Malmek E-M, Wismans J, Dávila A, Monfrino G, Storer D, Coma G, Schönwald C (2013) Advanced electric vehicle architectures. ELVA SCP0-GA-2010-265898

Lu H, Zhang N, Zhou X, Wang Y, Lu E (2017) Comprehensive design and optimization of an electric vehicle powertrain equipped with a two-speed dual-clutch transmission. Adv Mech Eng 9(1):1–13. https://doi.org/10.1177/1687814016683144

Luccarelli M, Matt DT, Spena PR, Lienkamp M (2014) Purpose design for electric cars parameters defining exterior vehicle proportions. In: Bozen-Bolzano Institutional Archieve (BIA), conference publications in science and technology, pp 1–7. http://hdl.handle.net/10863/232

Mahala MK, Deb A (2011) Development of transmission specifications for an electric vehicle. In: Chakrabarti A (eds) Research into design—supporting sustainable product development. Indian Institute of Science, Bangalore, India, Published by Research Publishing ISBN: 978-981-08-7721-7, pp 978–981

Maryniuk R (2017) Development of a modular urban electric vehicle. Master thesis, Master of Applied Science, Department of Mechanical Engineering, University of Waterloo

Mashhoodi B, van der Blij N (2021) Drivers' range anxiety and cost of new EV chargers in Amsterdam: a scenario-based optimization approach. Ann GIS 27(1):87–98. https://doi.org/10.1080/19475683.2020.1848921

May GJ, Davidson A, Monahov B (2018) Lead batteries for utility energy storage: a review. J Energy Storage 15:145–157

Mruzek M, Gajdáč I, Kučera Ľ, Gajdošík T (2014) The possibilities of increasing the electric vehicle range. Procedia Eng 192:621–625

Mruzek M, Gajdáč I, Kučera Ľ, Barta D (2016) Analysis of parameters influencing electric vehicle range. Procedia Eng 134:165–174. https://doi.org/10.1016/j.proeng.2016.01.056

Norrby P (2012) Prediction of coast-down test results. Master thesis, Chalmers University of Technology

Othaganont P, Assadian F, Auger DJ (2016) Multi-objective optimisation for battery electric vehicle powertrain topologies. J Automobile Eng 231:8. https://doi.org/10.1177/0954407016671275

Parkinson S (2016) Optimum gear ratios for an electric vehicle. Undergraduate J Math Model One + Two 7(1), Article 4. https://doi.org/10.5038/2326-3652.7.1.4875

Patel R, Kumar S (2017) Analysis of packaging issues in current electric vehicles. Int J Eng Res Appl 7(8, Part-I):50–55. ISSN: 2248–9622

Petersen P et al (2019) Validation of range estimation for electric vehicles based on recorded real-world driving data. In: Bargende M, Reuss HC, Wagner A, Wiedemann J (eds) 19 Internationales Stuttgarter symposium. Proceedings. Springer Vieweg, Wiesbaden. https://doi.org/10.1007/978-3-658-25939-6_29

Preda I, Covaciu D, Ciolan G (2010) Coast down test—theoretical and experimental approach. CONAT20104030, pp 155–162

Prochazka P, Pazdera I, Cipin R, Hadas Z (2015) Optimal design techniques for small electric car operating in common urban traffic. Brno University of Technology, PRZEGLĄD ELEKTROTECHNICZNY, ISSN 0033-2097, R. 91 NR 5/2015. https://doi.org/10.15199/48.2015.05.38

Richardson RR, Osborne MA, Howey DA (2018) Battery health prediction under generalized conditions using a Gaussian process transition model. J Energy Storage 23:320–328

Sankaran G, Venkatesan S, Prabhahar M (2020) Range anxiety on electric vehicles in India—impact on customers and factors influencing range anxiety. Mater Today—Proc 33(Part 1):895–901. https://doi.org/10.1016/j.matpr.2020.06.423

Saxena S, Gopal A, Phadke A (2020) Electrical consumption of two-, three- and four-wheel light-duty electric vehicles in India. Appl Energy 115(2014):582–590

Scheubner S, Thorgeirsson AT, Vaillant M, Gauterin F (2019) A stochastic range estimation algorithm for electric vehicles using traffic phase classification. IEEE Trans Veh Technol 68(7):6414–6428. https://doi.org/10.1109/TVT.2019.2918544

Sherman SB, Cano ZP, Fowler M, Chen Z (2018) Range-extending Zinc-air battery for electric vehicle. AIMS Energy 6(1):121–145

Shukla PR, Dhar S, Pathak M, Bhaskar K (2014) Electric vehicles scenarios and a roadmap for India. UNEP DTU Partnership

Singh NP, Chauhan H (2017) Dynamic analysis & shape optimization of electric car chassis. Int J Aerospace Mech Eng 4(4):5–8

Stein J, Urban P, Seidel K, Kerschbaumer A (2016) Epsilon—small electric passenger vehicle with maximized safety and integrating a lightweight oriented novel body architecture. FORMforum 1–10

Tanik E, Parlaktaş V (2015) Design of a very light L7E electric vehicle prototype. Int J Automot Technol 16(6):997–1005. https://doi.org/10.1007/s12239-015-0102-6

Taufik AZ, Rashid N, Faruq M, Mazlan, Zahir M (2014) Electric car chassis design and analysis by using CATIA V5 R19. IOSR J Mech Civil Eng (IOSR-JMCE) 11(4 Ver. III):56–59. e-ISSN: 2278-1684, p-ISSN: 2320-334X

Tsirogiannis EC, Stavroulakis GE, Makridis SS (2019) Electric car chassis for shell eco marathon competition: design, modelling and finite element analysis. World Electric Veh J 10:8. https://doi.org/10.3390/wevj10010008

Tutuianu M, Marotta A, Steven H, Ericsson E, Haniu T, Ichikawa N, Ishii H (2014) Development of a world-wide worldwide harmonized light duty driving test cycle (WLTC). Technical report, DHC subgroup", vol 03, no January, 7–10

Type I test On S.I. engines, CNG, LPG and diesel engine vehicles (Verifying the average tailpipe emission) of gaseous and particulate pollutants, Chapter 3, MoRTH/CMVR/TAP-115/116 (Issue 4), pp 895–918 (2018)

Wishart J, Diez J (2015) Test specification—coastdown testing. Intertek company, Center for Evaluation of Clean Energy Technology (CECET)

Wismans J, Malmek E-M, Larsson R, Welinder J, Håland Y, Oldenbo M (2011) Technology needs for Safe Electric Vehicle Solutions in 2030. https://www-esv.nhtsa.dot.gov/Proceedings/22/files/22ESV-000128.pdf

Xin X, Chengning Z (2017) Optimal design of electric vehicle power system with the principle of minimum curb mass. Energy Procedia 105:2629–2634

Yin Y, Yin X, Luo W, Sun H (2017) Comparison research of electric vehicles equipped with fixed ratio gearbox and two-speed gearbox. Int J Recent Adv Mech Eng (IJMECH) 6(2)

Zhou XX, Walker PD, Zhang N, Zhu B, Ding F (2012) The influence of transmission ratios selection on electric vehicle motor performance. In: Proceedings of the ASME 2012 international mechanical engineering congress & exposition IMECE2012, November 9-15, 2012, Houston, Texas, USA IMECE2012–85906